



Contents lists available at ScienceDirect

Journal of Theoretical Biology

journal homepage: www.elsevier.com/locate/yjtbi

Impact of plasma-protein binding on receptor occupancy: An analytical description

Lambertus A. Peletier^{a,*}, Neil Benson^b, Piet H. van der Graaf^b

^a Mathematical Institute, Leiden University, P.O. Box 9512, 2300 RA Leiden, The Netherlands

^b Pfizer Global Research & Development, Department of Pharmacokinetics, Dynamics and Metabolism, IPC 654, Sandwich CT13 9NJ, UK

ARTICLE INFO

Article history:

Received 16 June 2008

Received in revised form

5 August 2008

Accepted 3 September 2008

Keywords:

Plasma-protein binding

Receptor occupancy

Modelling complex systems behaviours

Time scales

Analytical descriptions

ABSTRACT

In this paper we analyse the dynamics of an inhibitor I which can either bind to a receptor R or to a plasma protein P . Assuming typical association and dissociation rates, we find that after an initial dose of inhibitor, there are three time scales: a *short* one, measured in fractions of seconds, in which the inhibitor concentration and the plasma-protein complex jump to quasi-stationary values, a *medium* one, measured in seconds in which the receptor complex rises to an equilibrium value and a *large* one, measured in hours in which the inhibitor-receptor complex slowly drops down to zero. We show that the average receptor occupancy, the pharmacologically relevant quantity, taken over, say, 24 h reaches a maximal value for a specific value of the plasma-protein binding constant. Potentially, understanding and exploiting this optimum could be of great interest to those involved in drug discovery and development.

© 2008 Elsevier Ltd. All rights reserved.

1. Introduction

Plasma-protein binding of small molecule drugs is viewed by many as a critical parameter in drug discovery. In large part this derives from the assumption that free drug alone can bind to target and elicit a pharmacodynamic response i.e., a drug cannot exert its action if it is bound to a large molecule such as a plasma protein. This is often referred to as the *free drug hypothesis* in the field of drug discovery (for more a detailed review, see Smith et al., 2006; Trainor, 2007).

The composition of human plasma is well documented and constitutes some 70 proteins (Putnam, 1984). Of these the most critical are held to be *human serum albumin* (HSA) (Jusko, 1976) and *alpha1-acid glycoprotein* (AGP) (Fournier et al., 2000). Both HSA and AGP have relatively high concentrations in human plasma. The concentration of HSA is 500–800 μM with multiple binding sites per molecule (Wanwimolruk et al., 1983) and the concentration of AGP is in the region of 12–31 μM in plasma (Israilli and Dayton, 2001).

Broadly speaking, different drugs bind preferentially to one or other of these: HSA tends to bind acidic or neutral drugs, whereas AGP binds neutral and basic molecules. Recently it has been shown that binding affinity for drug to plasma proteins such as

HSA can readily be measured (Rich et al., 2001; Frostell-Karlsson et al., 2000; Talbert et al., 2002; Schuhmacher et al., 2004). Furthermore, accurate estimates of free fraction can be derived using these affinity parameters and information about the concentration of these proteins, consistent with the hypothesis that binding to HSA and/or AGP dominates behaviour.

Despite the importance of plasma-protein binding, the wealth of knowledge about the interacting components and the solid basic principles embodied in the free drug hypothesis, the impact of such binding in a system is not well understood. There is a perception that high plasma-protein binding attenuates drug efficacy (Trainor, 2007), whilst there are numerous cases where highly bound drugs exhibit an apparently far greater effect than could plausibly be expected (Ericsson et al., 2004; Gerskowitch et al., 2007; Schäfer-Korting et al., 1995). In addition, plasma proteins such as HSA can be compartmentalised in the body (Oie and Tozer, 1979), leading to the potential for complex behaviours dependent on the physico-chemistry of the drug considered.

We believe that a mathematical approach is essential to achieving an understanding of these apparent non-intuitive behaviours and of the potential for complex system behaviours. In an elegant paper, Martin (1965), took such an approach to the pharmacokinetics of a hypothetical drug. The model proposed assumes that drug bound to a plasma protein and that only free (unbound) drug was available to be eliminated. This was described mathematically and it was shown that high affinity binding to plasma proteins could lead to non-intuitive behaviours, such as an apparent disconnect in the time course behaviour of drug in plasma versus that in total body water.

* Corresponding author. Tel.: +31 71 5146864; fax: +31 71 5140979.

E-mail addresses: peletier@math.leidenuniv.nl (L.A. Peletier),

Neil.Benson@pfizer.com (N. Benson), Piet.Van.Der.Graaf@pfizer.com (P.H. van der Graaf).

In the present paper, we extend this inquiry to include the impact of the drug binding to a plasma protein on the receptor occupancy of a drug target of interest. To simplify, we assume in the first instance that the drug is restricted to a single compartment (the plasma and interstitial fluid compartment), binds to a single plasma protein and has unrestricted access to the molecular target in that compartment. We also assume that the molecular target is in equilibrium at a low concentration (much less than one tenth) relative to drug and HSA, a commonly used assumption (cf. Kenakin, 2004).

The main objective of this study is to test the validity of the perception that high plasma-protein binding will necessarily attenuate receptor occupancy and therefore pharmacodynamic effect over the pharmacokinetic time course. Thus, we consider a compartment in which a drug, referred to as an “inhibitor”, binds to a plasma protein such as HSA and a target receptor to form an inhibitor–protein complex and an inhibitor–receptor complex. The parameters describing these interactions are routinely measured in drug discovery programmes. For example, plasma-protein binding kinetics can be readily measured using surface plasmon resonance (SPR) and Rich et al. suggest 300–400 compounds per week could be screened using this approach. Binding of drug to targets such as enzymes and receptors can also be routinely generated using well established techniques (Kenakin, 2004).

We shall follow the dynamics of this collection of compounds as time progresses, starting from an initial state in which there are only proteins, receptors and an initial dose of free inhibitor.

We shall focus on the receptor occupancy—the fraction of inhibitor–receptor complex over the total amount of receptor—this being the main determinant of drug efficacy, and study its dependence on the protein binding constant (K_P) and the rate (k_{out}) with which the free inhibitor is removed from the compartment.

Using the prior knowledge that molecular binding events tend to be rapid relative to physiological processes such as drug clearance, we shall be able to distinguish three different time scales and obtain explicit expressions for the receptor occupancy which are good approximations in the shorter, the medium and the large time development. Thanks to these explicit expressions we are able to obtain a detailed picture of the effect of plasma-protein binding and so test the commonly held perceptions about it.

2. The model

In order to study the impact of plasma-protein binding on receptor occupancy, we analyse a simple one-compartment model in which a drug, the inhibitor (I), binds reversibly not only to its target receptor (R) but also to a plasma protein (P) that is present in the compartment, to form complexes CR and CP , respectively. Whilst the inhibitor is introduced instantaneously at the outset, it subsequently slowly flows out of the compartment according to a first order process. Schematically this model is described by the following set of reaction equations:



and



in which P , CP , R , CR and I now denote the concentrations of these compounds (i.e., $P = [P]$, $CP = [CP]$, etc.), The values of k_1 and k_{-1} listed in Table 1 correspond to typical values for HSA (cf. Rich et al., 2001; Frostell-Karlsson et al., 2000). Those of k_2 and k_{-2} are typical for drug binding to receptor (cf. Kenakin, 2004), and the value of k_{out} represents rapid drug clearing in man.

Note that for these values

$$K_P = 10^2 \mu\text{M} \quad \text{and} \quad K_R = 10^{-4} \mu\text{M} \quad (2.4)$$

Our objective will be to see how varying the affinity K_P of the inhibitor to the plasma proteins in the range from $K_P = 0.1$ to $100 \mu\text{M}$, and the efflux rate k_{out} in the range $0.01 - 0.05 \text{ s}^{-1}$ affects the dynamics, and in particular the receptor occupancy, whilst we keep the rate constants k_2 and k_{-2} , and hence the affinity K_R of the inhibitor to the receptor, fixed. We shall do this first by changing k_1 and then by changing k_{-1} .

The dynamics of the above set of reactions is described by the following set of differential equations:

$$\begin{aligned} \frac{dP}{dt} &= -k_1 I \cdot P + k_{-1} CP \\ \frac{dCP}{dt} &= +k_1 I \cdot P - k_{-1} CP \\ \frac{dR}{dt} &= -k_2 I \cdot R + k_{-2} CR \\ \frac{dCR}{dt} &= +k_2 I \cdot R - k_{-2} CR \\ \frac{dI}{dt} &= -k_1 I \cdot P + k_{-1} CP - k_2 I \cdot R + k_{-2} CR - k_{out} I \end{aligned} \quad (2.5)$$

Initially, at $t = 0$, the inhibitor is supplied instantaneously to a clean compartment, i.e., prior to this infusion, the compartment was free from inhibitor. Thus, we have

$$P(0) = P_0, \quad R(0) = R_0, \quad I(0) = I_0, \quad CP(0) = 0, \quad CR(0) = 0 \quad (2.6)$$

where P_0 and R_0 are the initial concentrations of plasma proteins and receptors and I_0 is the drug concentration just after the infusion. Realistic values of these initial data are given in Table 2 (cf. Kenakin, 2004).

Two Conservation Laws are readily derived from the system (2.5), one for the plasma proteins and one for the receptors. They remain in the compartment for all time. Thus, the total amount of protein in the compartment, free or bound, is constant over time, so that

$$P(t) + CP(t) = P_0 \quad \text{for } 0 \leq t < \infty \quad (2.7)$$

and similarly, the total amount of receptor in the compartment, free or bound, is constant over time, so that

$$R(t) + CR(t) = R_0 \quad \text{for } 0 \leq t < \infty \quad (2.8)$$

Table 1 Rate constants

$k_1 (\mu\text{M}^{-1} \text{ s}^{-1})$	$k_{-1} (\text{ s}^{-1})$	$k_2 (\mu\text{M}^{-1} \text{ s}^{-1})$	$k_{-2} (\text{ s}^{-1})$	$k_{out} (\text{ s}^{-1})$
10	10^3	10	10^{-3}	2×10^{-2}

Table 2 Initial values (all in μM)

P_0	I_0	R_0
750	0.1	10^{-3}

These conservation laws enable us to eliminate $P(t)$ and $R(t)$ from the system (2.5) and so reduce it to a system of three ordinary differential equations:

$$\frac{dCP}{dt} = +k_1P_0I - (k_1I + k_{-1})CP$$

$$\frac{dCR}{dt} = +k_2R_0I - (k_2I + k_{-2})CR$$

$$\frac{dI}{dt} = -(k_1P_0 + k_2R_0 + k_{out})I + (k_1I + k_{-1})CP + (k_2I + k_{-2})CR \quad (2.9)$$

In order to acquire a first impression of the structure of the dynamics of this system, its time scales and its short, medium and large time behaviour, we carry out a brief numerical study and present a few typical concentration profiles of the complexes and the inhibitor.

3. Simulations

Exploring the effect of plasma-protein binding on the dynamics, and in particular the time course, of the receptor occupancy of the inhibitor, we first present graphs of the inhibitor-receptor complex concentration $CR(t)$ versus time for

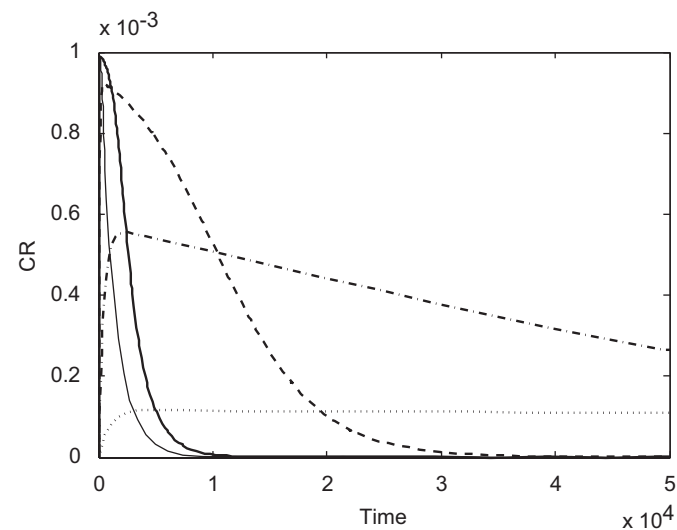


Fig. 1. Graph of the receptor complex concentration $CR(t)$ versus time for $K_p = 100$ (solid), 10 (dashed), 1 (dash-dot), 0.1 (dotted) μM , as well as in the absence of protein, $k_1 = 0$ (thin and solid). The constants are given in Table 1, except for the rate constant k_{-1} which runs from 10^3 s^{-1} ($K_p = 100 \mu\text{M}$) to 10^{-1} s^{-1} ($K_p = 0.1 \mu\text{M}$). The initial values of the five compounds are given in (2.6) and Table 2. Time is measured in seconds (12 h = 43 200 s).

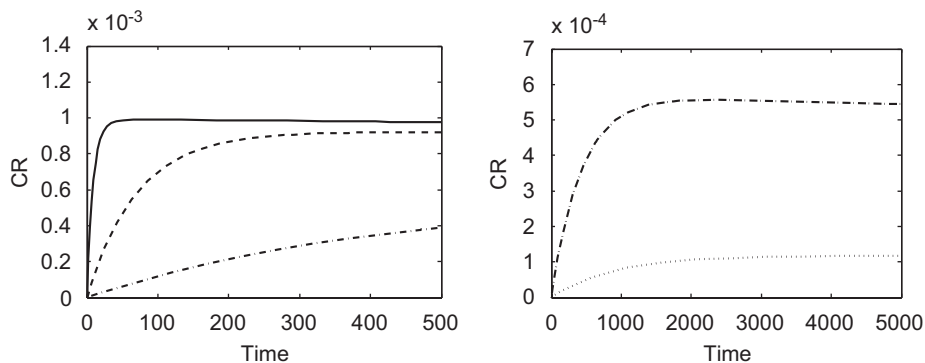


Fig. 2. Graph of $CR(t)$ for $K_p = 100 \mu\text{M}$ (solid), $K_p = 10 \mu\text{M}$ (dashed) and $K_p = 1 \mu\text{M}$ (dash-dot) and $K_p = 0.1 \mu\text{M}$ (dotted)—time in seconds.

four values of the protein binding constant K_p . The value of K_p ranges from a large value ($K_p = 100 \mu\text{M}$), when the tendency to associate is relatively small, to a small value ($K_p = 0.1 \mu\text{M}$), when the tendency to associate is large. The efflux rate k_{out} is kept fixed at 0.02 s^{-1} . The four graphs of $CR(t)$ are shown in Fig. 1.

Initially, the graphs in Fig. 1 all exhibit a rapid rise of the receptor occupancy toward a maximum and then a relatively gentle decline to zero. In Fig. 2 we present a blow-up of the graphs of $CR(t)$ over this initial period.

Over the larger time interval it is evident from the graphs of Fig. 1 that as K_p decreases, the receptor occupancy decreases in the short term but increases over a longer time span. This suggests that an integrated measure of the reactor occupancy, such as the area under the curve AUC over a suitable period of time T , say $T = 24 \text{ h}$, is appropriate here:

$$AUC(T) = \int_0^T \frac{CR(t)}{R_0} dt \quad (3.1)$$

In Fig. 3 we exhibit the AUC over 24 h as a function of the protein binding constant K_p and the elimination rate $k_{out} = 0.02 \text{ s}^{-1}$. The dots denote values of the AUC which have been computed numerically, whilst the solid curve is a graph of the theoretically derived approximation of the AUC given by (7.18). We see that for this choice of k_{out} , the AUC assumes its maximum value for a positive value of the protein-plasma binding constant K_p .

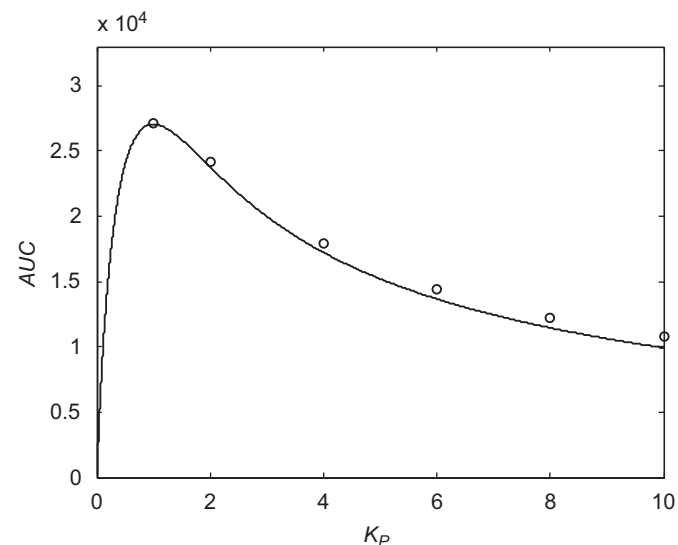


Fig. 3. Area under the curve defined by (3.1) for $T = 24 \text{ h}$, as a function of K_p , for $0 < K_p \leq 10 \mu\text{M}$. The dots denote numerically computed values; the solid curve represents the approximate values computed by means of (7.18).

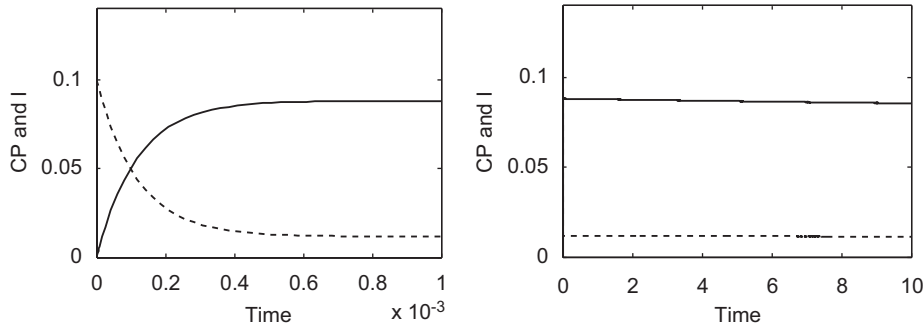


Fig. 4. Graphs of $CP(t)$ (solid) and $I(t)$ (dashed) on short (left) and medium (right) time scale for $K_p = 10 \mu\text{M}$ and $k_{out} = 0.02 \text{ s}^{-1}$; time in seconds.

The bell-shaped AUC versus K_p graph illustrates that receptor binding is impaired for high and low values of K_p : at very low values of K_p , plasma-protein binding dominates and no free drug is available for receptor binding whereas at very high values of K_p clearance of the drug dominates and drug is removed from the plasma compartment before it can bind to the receptor. As a result, an optimum exists for an intermediate value of K_p , the location of which is explored further in the Discussion (Fig. 7).

For completeness, we also present in Fig. 4 the time course of the concentrations of the inhibitor-protein complex CP and the free inhibitor I for the short and the medium time scale. Here $K_p = 10 \mu\text{M}$ and $k_{out} = 0.02 \text{ s}^{-1}$.

In our analysis we shall be able to obtain explicit expressions which are very good approximations to the solutions of the system (2.9).

4. Dimensionless variables

In order to simplify the equations and identify the combinations of parameters which determine the dynamics of the system, we introduce dimensionless variables. First, we define the dimensionless concentrations:

$$x = \frac{CP}{P_0}, \quad y = \frac{CR}{R_0}, \quad z = \frac{I}{I_0} \quad (4.1)$$

where we have taken as reference values the initial concentrations of the free plasma proteins, the free receptors and the inhibitor at the onset. In terms of x , y and z the system (2.9) becomes

$$\begin{cases} \frac{dx}{dt} = +k_1 I_0 z - (k_1 I_0 z + k_{-1}) x \\ \frac{dy}{dt} = +k_2 I_0 z - (k_2 I_0 z + k_{-2}) y \\ \frac{dz}{dt} = -(k_1 P_0 + k_2 R_0 + k_{out}) z + (k_1 I_0 z + k_{-1}) \frac{P_0}{I_0} x + (k_2 I_0 z + k_{-2}) \frac{R_0}{I_0} y \end{cases} \quad (4.2)$$

As was evident in Section 3, in the temporal evolution of the three concentrations we can distinguish three time scales, a short one, a medium one and a large one. We shall see that the short one is dictated by the time scale with which the inhibitor binds to the plasma proteins i.e., by the rate constant k_{-1} . Thus, for studying the short time behaviour of the system, we introduce the dimensionless time

$$\tau_1 = k_{-1} t \quad (4.3)$$

It will prove convenient to continue using this time scale for the behaviour on the medium time scale.

For the large time behaviour of the system we turn to the rate k_{-2} at which the inhibitor binds to the receptor and we employ

the time variable

$$\tau_2 = k_{-2} t \quad (4.4)$$

and an even larger time scale

$$\tau_3 = \kappa \tau_2 = \kappa k_{-2} t, \quad \text{where } \kappa = \frac{K_p}{P_0} \quad (4.5)$$

5. The short time behaviour

As we shall see, the short time behaviour is dictated by the plasma-protein binding for which k_{-1} is a characteristic rate. This motivates using the dimensionless time $\tau_1 = k_{-1} t$ as defined by (4.3). Introducing this new time variable in the system (4.2), we obtain

$$\begin{cases} \frac{dx}{d\tau_1} = \frac{k_1 I_0 z}{k_{-1}} - \left(\frac{k_1 I_0 z}{k_{-1}} + 1 \right) x \\ \frac{dy}{d\tau_1} = \frac{k_{-2}}{k_{-1}} \left\{ \frac{k_2 I_0 z}{k_{-2}} - \left(\frac{k_2 I_0 z}{k_{-2}} + 1 \right) y \right\} \\ \frac{dz}{d\tau_1} = \left(\frac{k_1 I_0 z}{k_{-1}} + 1 \right) \frac{P_0}{I_0} x + \frac{k_{-2}}{k_{-1}} \left(\frac{k_2 I_0 z}{k_{-2}} + 1 \right) \frac{R_0}{I_0} y \\ \quad - \frac{1}{k_{-1}} (k_1 P_0 + k_2 R_0 + k_{out}) z \end{cases} \quad (5.1)$$

This system suggests we define the following dimensionless quantities:

$$a \stackrel{\text{def}}{=} \frac{k_1 I_0}{k_{-1}} = \frac{I_0}{K_p}, \quad b \stackrel{\text{def}}{=} \frac{k_2 I_0}{k_{-2}} = \frac{I_0}{K_R} \quad \text{and} \quad \varepsilon \stackrel{\text{def}}{=} \frac{k_{-2}}{k_{-1}} \quad (5.2)$$

For the parameter values given in Tables 1 and 2, we find for a , b and ε : and

$$b = 10^3, \quad \varepsilon = 10^{-6} \quad \text{if } k_{-1} = 10^3 \text{ s}^{-1}$$

Introducing these constants into (5.1) we obtain

$$\begin{cases} \frac{dx}{d\tau_1} = az - (az + 1)x \\ \frac{dy}{d\tau_1} = \varepsilon \{ bz - (bz + 1)y \} \\ \frac{dz}{d\tau_1} = (az + 1) \frac{P_0}{I_0} x + \varepsilon (bz + 1) \frac{R_0}{I_0} y - \left(a \frac{P_0}{I_0} + \varepsilon b \frac{R_0}{I_0} + \frac{k_{out}}{k_{-1}} \right) z \end{cases} \quad (5.3)$$

Plainly, in light of (2.6) and (4.1) the initial values are now

$$x(0) = 0, \quad y(0) = 0 \quad \text{and} \quad z(0) = 1 \quad (5.4)$$

The question as to the impact of plasma-protein binding on receptor occupancy now translates to the effect of the binding constant K_p on the dynamics of the system (5.3). In varying K_p we first vary k_1 and keep k_{-1} fixed, because in this case ε remains constant and only $a = I_0/K_p$ will change. We then turn to the case in which the roles of k_1 and k_{-1} are reversed, and k_{-1} changes whilst k_1 is kept fixed.

5.1. k_{-1} fixed and k_1 varies

We put $k_{-1} = 10^3 \text{ s}^{-1}$. Then $\varepsilon = 10^{-6}$ and this is such a small quantity, that we may approximate the system (5.3) by a much simpler system when discussing the dynamics on a time scale of order unity. In Appendix A we shall show that for a time span of $0 < \tau_1 < T_1(\varepsilon)$, where $T_1(\varepsilon)$ is of order unity, the solution of Problem (5.3), (5.4) is well approximated by the solution of the *reduced system*

$$\begin{cases} \frac{dx}{d\tau_1} = az - (az + 1)x \\ \frac{dy}{d\tau_1} = 0 \\ \frac{dz}{d\tau_1} = (az + 1)\frac{P_0}{I_0}x - a\frac{P_0}{I_0}z \end{cases} \quad (5.5)$$

in which all the terms in (5.3) involving ε have been dropped and the loss term involving k_{out} has also been omitted because it is small compared to k_{-1} . In light of the initial conditions (5.4) we conclude that

$$y(\tau_1) = 0 \quad \text{for } \tau_1 \geq 0 \quad (5.6)$$

The two remaining concentrations $x(\tau_1)$ and $z(\tau_1)$ are then determined by the two-dimensional system

$$\begin{cases} \frac{dx}{d\tau_1} = az - (az + 1)x \\ \frac{dz}{d\tau_1} = (az + 1)\frac{P_0}{I_0}x - a\frac{P_0}{I_0}z \end{cases} \quad (5.7)$$

together with the initial conditions $x(0) = 0$ and $z(0) = 1$.

The system (5.7) has a special structure: when we multiply the second equation by I_0/P_0 and add the resulting equation to the first equation, we obtain

$$\frac{dx}{d\tau_1} + \frac{I_0}{P_0} \frac{dz}{d\tau_1} = \frac{d}{d\tau_1} \left(x + \frac{I_0}{P_0} z \right) = 0 \quad \text{for } \tau_1 \geq 0$$

Hence $x + (I_0/P_0)z$ is a constant of motion. In view of the initial conditions $(x, y, z) = (0, 0, 1)$, we conclude that

$$x(\tau_1) + \frac{I_0}{P_0} z(\tau_1) = \frac{I_0}{P_0} \quad \text{for } \tau_1 \geq 0 \quad (5.8)$$

Note that when we multiply this identity by P_0 , and return to the original variables, we obtain the relation

$$CP(t) + I(t) = I_0 \quad \text{for } \tau_1 \geq 0$$

which states that in the compartment the inhibitor is either free, or bound to the plasma protein, i.e., the amount that is bound to the receptor is negligible.

We can use (5.8) to eliminate $x(\tau_1)$ from the second equation in (5.7). This yields a single differential equation in z :

$$\frac{dz}{d\tau_1} = f(z) \stackrel{\text{def}}{=} (az + 1)(1 - z) - a\frac{P_0}{I_0}z \quad (5.9)$$

We find that $f(z)$ has a unique positive zero \bar{z} and it is readily seen that

$$z(\tau_1) \rightarrow \bar{z} \quad \text{as } \tau_1 \rightarrow \infty \quad (5.10)$$

From the conservation law (5.8) we immediately deduce that

$$x(\tau_1) \rightarrow \bar{x} \stackrel{\text{def}}{=} \frac{I_0}{P_0} (1 - \bar{z}) \quad \text{as } \tau_1 \rightarrow \infty \quad (5.11)$$

For the parameter values of Tables 1 and 2 and for K_P between 0.1 and $100 \mu\text{M}$,

$$\bar{z} \approx \frac{K_P}{K_P + P_0} = \frac{\kappa}{\kappa + 1} \quad \text{and} \quad \bar{x} \approx \frac{I_0}{P_0} \frac{1}{\kappa + 1}, \quad \kappa = \frac{K_P}{P_0} \quad (5.12)$$

In what follows, the dimensionless parameter $\kappa = k_{-1}/(k_1 P_0)$ will play an important role. We therefore give here some numerical values (Table 4).

Thus, for $K_P \leq 10$ we may view κ as a small quantity.

In order to estimate the rate of convergence in the limits in (5.10) and (5.11), we need to compute df/dz at \bar{z} . We find

$$\left. \frac{df}{dz} \right|_{z=\bar{z}} \approx \frac{\kappa + 1}{\kappa}.$$

This means that the half life $\tau_{1,1/2}$ of $z(\tau_1) - \bar{z}$ is equal to

$$\tau_{1,1/2} \approx \frac{\kappa}{\kappa + 1} \ln 2 \leq \kappa \ln 2 < 0.1 \quad \text{if } K_P \leq 100 \quad (5.13)$$

This means that $\tau_{1,1/2} = O(1)$, so that the reduction of the full system (5.3) to the simpler system is indeed justified (Tables 3 and 4).

In conclusion, we see that after a few microseconds $x(t)$ and $z(t)$ have each reached a plateau value where they stay for a while, and $y(t)$ has not really changed from its initial value $y(0) = 0$. Thus, over the initial interval

$$x(t) \rightarrow \bar{x}, \quad y \approx 0 \quad \text{and} \quad z(t) \rightarrow \bar{z} \quad (5.14)$$

These plateau values \bar{x} and \bar{z} are the *equilibrium values* of x and z in the absence of receptors and clearance. For completeness we give in Table 5 the numerical values of \bar{x} and \bar{z} for four values of K_P .

5.2. k_1 fixed and k_{-1} varies

We fix $k_1 = 10 \mu\text{M}^{-1} \text{ s}^{-1}$ and vary k_{-1} in the range $10^3 - 1 \text{ s}^{-1}$. If k_{-1} decreases through this range then ε increases from 10^{-6} to 10^{-3} s^{-1} and K_P decreases from 100 to $0.1 \mu\text{M}$.

In Appendix A we show that, as in Section 5.1, the dynamics of $x(\tau_1)$ and $z(\tau_1)$ is still well described by the system (5.7):

$$\begin{cases} \frac{dx}{d\tau_1} = az - (az + 1)x \\ \frac{dz}{d\tau_1} = (az + 1)\frac{P_0}{I_0}x - a\frac{P_0}{I_0}z \end{cases} \quad (5.7)$$

Table 3
Values of the parameter a in the system (5.1)

K_P	0.1	1	10	100
a	1	0.1	0.01	0.001

Table 4
Values of κ

K_P	0.1	1	10	100
κ	1.3×10^{-4}	1.3×10^{-3}	0.013	0.13

Table 5
Plateau values \bar{x} and \bar{z}

K_P	0.1	1	10	100
\bar{x}	1.333×10^{-4}	1.332×10^{-4}	1.316×10^{-4}	1.176×10^{-4}
\bar{z}	1.335×10^{-4}	1.331×10^{-3}	1.316×10^{-2}	1.176×10^{-1}

Table 6
Plateau values \bar{y}

K_P	0.1	1	10	100
\bar{y}	0.118	0.57	0.93	0.99

over a time span of $\tau_1 = O(1)$. Here we have merely assumed that $0 \leq y \leq 1$.

Since ε may now be as large as 10^{-3} and $b = 10^3$, we see that the right-hand side of the second equation, $\varepsilon\{bz - (bz + 1)y\}$, no longer needs to be small. Hence, in this scenario the second equation in the system (5.3) cannot be replaced by $dy/d\tau_1 = 0$.

6. The medium time behaviour

In Section 5 we have seen that within a very short time, $x(\tau_1)$ and $z(\tau_1)$ reach plateau values \bar{x} and \bar{z} . In this section we show that on a somewhat larger time scale $y(\tau_1)$ also reaches a plateau value \bar{y} . We assume that on this "medium time scale", $x(\tau_1)$ and $z(\tau_1)$ remain approximately constant, and so that \bar{x} and \bar{z} are good approximations of $x(\tau_1)$ and $z(\tau_1)$. We shall show a posteriori that this assumption is justified. This is done in Appendix B.

Thus, the medium time scale is the time scale on which inhibitor binds to receptor whilst inhibitor and protein are approximately in equilibrium.

Replacing $x(\tau_1)$ and $z(\tau_1)$ by, respectively, \bar{x} and \bar{z} , we find that $y(\tau_1)$ is determined by the initial value problem

$$\frac{dy}{d\tau_1} = \varepsilon\{b\bar{z} - (b\bar{z} + 1)y\}, \quad y(0) = 0 \tag{6.1}$$

where we have taken the initial condition from (5.14). This problem admits an explicit solution:

$$y(\tau_1) = \frac{b\bar{z}}{b\bar{z} + 1} (1 - e^{-\varepsilon(b\bar{z} + 1)\tau_1}) \tag{6.2}$$

Plainly,

$$y(\tau_1) \rightarrow \bar{y} = \frac{b\bar{z}}{b\bar{z} + 1} \quad \text{as } \tau_1 \rightarrow \infty \tag{6.3}$$

i.e., $y(\tau_1)$ also reaches a plateau value \bar{y} , and this happens on a time scale of

$$\tau_{1,1/2}^* = \frac{\ln 2}{\varepsilon(b\bar{z} + 1)} \tag{6.4}$$

which ranges from 6×10^3 ($K_p = 100 \mu\text{M}$) to 6×10^5 ($K_p = 0.1 \mu\text{M}$) i.e., from 6 to 600 s.

Thus, after a medium time interval of several seconds or minutes, depending on the value of K_p , we have

$$x \approx \bar{x}, \quad y \approx \bar{y} \quad \text{and} \quad z \approx \bar{z} \tag{6.5}$$

In Table 6 we present values of \bar{y} for four values of K_p .

7. The large time behaviour

The large time behaviour is determined by the binding of inhibitor to both protein and receptor, as well as its degradation over time. As a first step towards determining the correct rate of decay, we select a time scale that is based on the inhibitor-receptor binding and hence we multiply the time variable t by the rate constant k_{-2} :

$$\tau_2 = k_{-2}t, \quad (k_{-2} = 10^{-3} \text{ s}^{-1})$$

When we transform the system (4.2) to this time scale, we obtain

$$\begin{cases} \varepsilon \frac{dx}{d\tau_2} = az - (az + 1)x \\ \frac{dy}{d\tau_2} = bz - (bz + 1)y \\ \frac{dz}{d\tau_2} = \frac{1}{\varepsilon} \frac{P_0}{I_0} (az + 1)x + v(bz + 1)y - \left(\frac{1}{\varepsilon} \frac{aP_0}{I_0} + b \frac{R_0}{I_0} + \frac{k_{out}}{k_{-2}} \right) z, \end{cases} \tag{7.1}$$

and we take as initial values

$$x(0) = \bar{x}, \quad y(0) = \bar{y} \quad \text{and} \quad z(0) = \bar{z} \tag{7.2}$$

It will be convenient to introduce the variable

$$w = z + \frac{P_0}{I_0} x \tag{7.3}$$

Note that $I_0 w = I_0 + P_0 x = I + CP$ is the total amount of inhibitor in the compartment. As we saw in Eq. (5.8), this quantity is effectively constant on the short and medium time scale, when the loss of inhibitor from the compartment is neglected. Of course, this loss can no longer be ignored on a larger time scale.

If we multiply the first equation of the system (7.1) by $P_0/(\varepsilon I_0)$ and add the result to the third equation we obtain the system

$$\begin{cases} \varepsilon \frac{dx}{d\tau_2} = az - (az + 1)x \\ \frac{dy}{d\tau_2} = bz - (bz + 1)y \\ \frac{dw}{d\tau_2} = \frac{R_0}{I_0} (bz + 1)y - \left(b \frac{R_0}{I_0} + \frac{k_{out}}{k_{-2}} \right) z \end{cases} \tag{7.4}$$

This is once again a singular perturbation problem. By putting $\varepsilon = 0$ in (7.4) we formally obtain a relation between x and z :

$$0 = az - (az + 1)x \tag{7.5}$$

Since the initial data (\bar{x}, \bar{z}) satisfy this relation we may assume that it is satisfied for all time $\tau_2 \geq 0$. Note that (7.5) allows us to express x in terms of z :

$$x = \frac{az}{az + 1} \implies w = z + \frac{P_0}{I_0} \frac{az}{az + 1} \stackrel{\text{def}}{=} \psi(z)$$

Using these expressions to eliminate x and w from the third equation in (7.4), we obtain the following system for y and z :

$$\begin{cases} \frac{dy}{d\tau_2} = bz - (bz + 1)y \\ \psi'(z) \frac{dz}{d\tau_2} = \frac{R_0}{I_0} (bz + 1)y - \left(b \frac{R_0}{I_0} + \frac{k_{out}}{k_{-2}} \right) z \end{cases} \tag{7.6}$$

where

$$\psi(z) = z + \frac{P_0}{I_0} \frac{az}{az + 1} \tag{7.7}$$

It can readily be seen from a phase plane analysis of the system (7.6) that $z(\tau_2) \leq \bar{z}$ (cf. Appendix C). Therefore,

$$az(\tau_2) \leq a\bar{z} = \frac{I_0 K_p}{K_p P_0} = \frac{I_0}{P_0} \ll 1$$

Hence, we can approximate $\psi(z)$ by the function

$$\psi(z) = z + \frac{P_0}{I_0} az = (1 + \kappa^{-1})z \tag{7.8}$$

so that

$$\psi'(z) = 1 + \kappa^{-1}$$

Recall that $1/\kappa \geq 75$ if $K_p \leq 10 \mu\text{M}$. Hence for such values of K_p we may replace $\psi'(z)$ in (7.6) by $1/\kappa$.

It is now natural to introduce a third time scale

$$\tau_3 = \kappa \tau_2 = \kappa k_{-2} t \tag{7.9}$$

With this time variable, and the assumption that $K_p \leq 10 \mu\text{M}$, we may write the system (approximately) as

$$\begin{cases} \kappa \frac{dy}{d\tau_3} = bz - (bz + 1)y \\ \frac{dz}{d\tau_3} = v(bz + 1)y - (bv + \theta)z \end{cases} \quad v = \frac{R_0}{I_0}, \quad \theta = \frac{k_{out}}{k_{-2}} \tag{7.10}$$

Since $\kappa \ll 1$ this is yet another singular perturbation problem. It permits a reduction to the system

$$\begin{cases} 0 = bz - (bz + 1)y \\ \frac{dz}{d\tau_3} = v(bz + 1)y - (bv + \theta)z \end{cases} \quad (7.11)$$

Recall that the orbit starts at the point (\bar{y}, \bar{z}) which satisfies the first equation in (7.11). Using this equation to eliminate y from the second equation, we obtain an initial value problem for the single variable z :

$$\frac{dz}{d\tau_3} = -\theta z \quad \text{and} \quad z(0) = \bar{z} \quad (7.12)$$

Here, we have neglected the initial time interval in which $z(t)$ drops from 1 to \bar{z} . Since this interval only lasts a few milli-seconds, this is justified. We readily obtain the solution

$$z(\tau_3) = \bar{z}e^{-\theta\tau_3} \quad \text{for} \quad \tau_3 \geq 0$$

or, in terms of the original time variable, since $\theta = \theta\kappa k_{-2}$
 $t = \kappa k_{out} t$,

$$z(t) = \bar{z}e^{-\kappa k_{out} t} \quad \text{for} \quad t \geq 0 \quad (7.13)$$

In light of the first equation in (7.11) this yields for $y(t)$:

$$y(t) = \frac{b\bar{z}e^{-\kappa k_{out} t}}{1 + b\bar{z}e^{-\kappa k_{out} t}} = \frac{b\bar{z}}{b\bar{z} + e^{+\kappa k_{out} t}} \quad (7.14)$$

Thus, we have obtained explicit approximations for the temporal behaviour of the different compounds involved. In Fig. 5 we compare these approximations with the numerically obtained curves shown in Fig. 1. We see that, as expected, the approximation improves as K_p decreases and is already reasonable for $K_p = 10 \mu\text{M}$ and excellent when $K_p = 1$ and $0.1 \mu\text{M}$.

The approximate expression for $y(t)$ enables us to compute the AUC of the receptor occupancy (cf. (3.1)) over a given period of time $0 < t < T$:

$$AUC(T) = \int_0^T y(t) dt = \frac{1}{\kappa k_{out}} \ln \left(\frac{1 + b\bar{z}}{1 + b\bar{z}e^{-\kappa k_{out} T}} \right) \quad (7.15)$$

Note that if we allow for the time to be arbitrary large, i.e., $T = \infty$, this expression simplifies to

$$AUC(\infty) = \int_0^\infty y(t) dt = \frac{1}{\kappa k_{out}} \ln(1 + b\bar{z}) \quad (7.16)$$

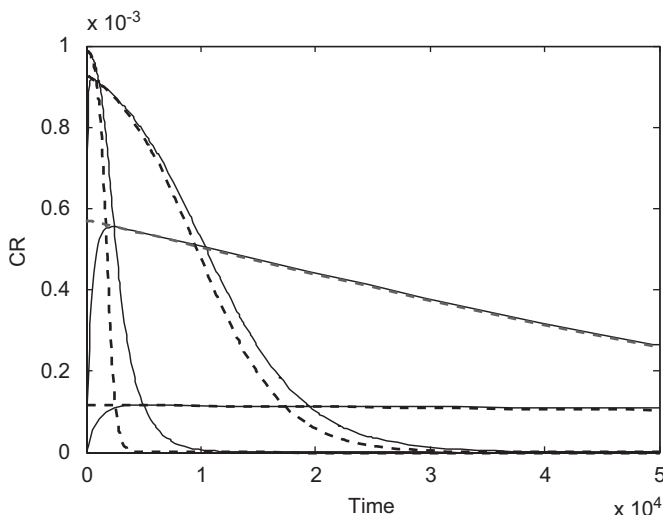


Fig. 5. Comparison of the numerically computed curves for $CR(t)$ shown in Fig. 1 (solid) with approximations obtained in (7.14) (dashed); $K_p = 0.1, 1, 10, 100 \mu\text{M}$ and $k_{out} = 0.02 \text{ s}^{-1}$; time t in seconds.

Table 7
Area under the curve over 24 h (cf. Fig. 3)

K_p	0.1	1	10
AUC—according to (7.18)	9200	27060	9941
AUC—numerically computed	9097	27118	10747

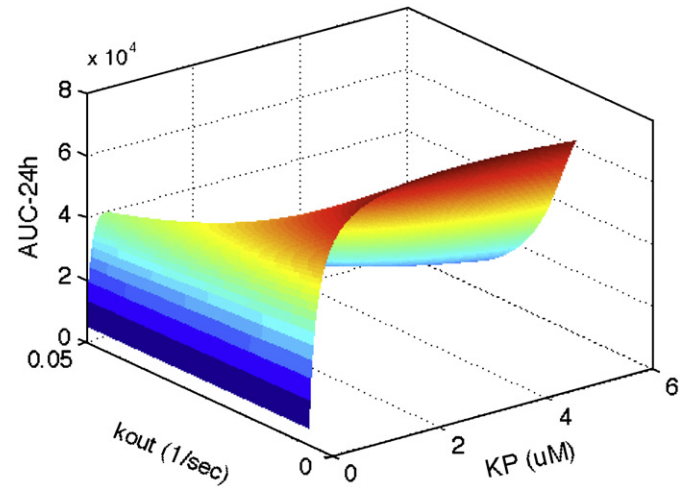


Fig. 6. Area under the curve of the receptor occupancy CR/R_0 for a 24 h period for different values of K_p and k_{out} , as computed by (7.18).

Using the expression (5.12) for \bar{z} ,

$$\bar{z}(\kappa) = \frac{\kappa}{1 + \kappa}$$

we can express the AUC as a function of κ and T . We obtain:

$$\begin{aligned} AUC(\kappa, T) &= \frac{1}{\kappa k_{out}} \ln \left(\frac{1 + b \frac{\kappa}{1 + \kappa}}{1 + b \frac{\kappa}{1 + \kappa} e^{-\kappa k_{out} T}} \right) \\ &= \frac{1}{\kappa k_{out}} \ln \left(\frac{1 + \kappa(1 + b)}{1 + \kappa(1 + b e^{-\kappa k_{out} T})} \right) \end{aligned} \quad (7.17)$$

Since $\kappa = K_p/P_0$, we obtain AUC, in terms of the constant K_p , P_0 and b :

$$AUC(K_p, T) = \frac{P_0}{K_p k_{out}} \ln \left(\frac{P_0 + K_p(1 + b)}{P_0 + K_p(1 + b e^{-K_p k_{out} T/P_0})} \right), \quad b = \frac{I_0}{K_R} \quad (7.18)$$

In Table 7 we give the values of $AUC(T)$ for $T = 24 \text{ h}$ ($T = 86400 \text{ s}$) for three values of the plasma-protein binding constant K_p (see also Fig. 3). Plainly, AUC is not a monotone function of K_p , and has an interior maximum.

In Fig. 6 we exhibit the AUC over 24 h as a function of the protein binding constant K_p and the elimination rate k_{out} . We see that for any given k_{out} , the graph of AUC versus K_p indeed has an interior maximum.

8. Discussion

We find that for typical values of association and dissociation rate constants a typical inhibitor binds very quickly to a plasma protein ($t_{1/2} = O(10^{-3}) \text{ s}$) and more slowly to a receptor ($t_{1/2} = O(1) \text{ s}$). According to Eq. (7.13), subsequent dissociation of inhibitor and receptor is much slower and ranges from $t_{1/2} = O(10^3) \text{ s}$ to $t_{1/2} = O(10^6) \text{ s}$ as the plasma-protein binding constant $K_p = k_{-1}/k_1$ varies from 100 to $0.1 \mu\text{M}$.

This wide disparity in time scales makes it possible to obtain explicit expressions which provide good approximations to the dynamic behaviour of all the compounds involved, and so enables one to study in detail the impact of proteins in the plasma on the effectiveness of drugs that are injected into the plasma.

We find that, measured over a specific time interval, the impact of plasma-protein binding does not increase *monotonically* as the binding constant K_P decreases. Specifically, if we measure the efficacy of an inhibitor by its receptor occupancy $y = CR/R_0$, then we find that the area under the curve AUC of $y(t)$ taken over a 24 h period first rises and then drops as K_P decreases from 10 to 0.1 μM , i.e., there exists a value of K_P where the receptor occupancy is optimal.

As K_P , K_R and in many cases a good estimate of k_{out} can be determined and data exist for typical reactant concentrations, one potentially attractive application of the calculations outlined in this paper is the selection of optimal compounds for progression in drug discovery programmes; with the parameters as inputs, the analytical approximations derived here allow a response surface to be calculated as shown in Fig. 6. Hence, the properties of candidate molecules can be rapidly compared and the optimal molecules selected.

The k_{on} and k_{off} rates of the inhibitor (drug) which we have used in this paper are typical. However, there is a spectrum of rate values (cf. Copeland et al., 2006). This model provides a convenient instrument with which the impact of variations of these rate constants can be explored.

We also see a number of potentially useful applications of this model to better understand commonly observed, but apparently non-intuitive observations; one important example is the impact of drug–drug interactions due to plasma-protein binding displacement. There has been a considerable debate about the clinical relevance of plasma-protein binding displacement interactions and there are only very few clinically important examples of drug–drug interactions due to this mechanism (Sansom and Evans, 1995; Jusko, 1976; Benet and Hoener, 2002). The contour plot in Fig. 7 provides some additional theoretical arguments to the ones outlined by Sansom and Evans, 1995 and Jusko, 1976, why this may be the case. Assuming a simple competitive interaction at the plasma protein P , the effect of the presence of a second drug would be an increase in the apparent value of K_P of the inhibitor, I . Thus, the effect on the AUC for receptor occupancy

can be visualised by a horizontal shift across the contour plot in Fig. 7 at a given value of k_{out} , which is assumed to be unchanged by the presence of the second drug. The parameter space for the simulations on which Fig. 7 is based was chosen to illustrate realistic scenarios of compounds that produce a meaningful pharmacological effect (i.e. >20% target occupancy) over a considerable period of time (i.e. 12 h), representing drugs that would typically be dosed once or twice daily. Overall, behaviour of the first compound and the impact of a second drug displacing it from P can be mapped onto one of the four regions shown in Fig. 7.

Region 1 comprises of compounds which display very high plasma-protein binding ($K_P < 0.75 \mu\text{M}$). In this region, very limited receptor occupancy will be observed irrespective of k_{out} . Increasing K_P would always lead to an increase in the AUC , however it is unlikely that this scenario will be encountered very often in clinical practise since compounds which display such limited intrinsic pharmacological activity would rarely be progressed as drug candidates.

Region 2 represents compounds which display high intrinsic clearance ($k_{out} > 0.0125/\text{s}$) and are relatively insensitive to increases in K_P . It can be seen that the most probable effect of increasing K_P is either no marked effect on the AUC (in particular in the green region at the upper half of the plot) or a transition to a region with a lower AUC (i.e. from yellow→green→blue), which at least from a safety point of view would not result in a drug–drug interaction of clinical concern.

Region 3 defines compounds with low intrinsic clearance ($k_{out} < 0.01/\text{s}$) and low plasma-protein binding ($K_P > 3 \mu\text{M}$). These compounds always yield high AUC 's (>75%) and the window for further increase due to increased K_P values is limited and in most cases unlikely to be clinically relevant. The only area of concern with respect to potential for drug–drug interactions is defined by Region 4.

Region 4 contains compounds with low intrinsic clearance ($k_{out} < 0.015/\text{s}$) and moderate plasma-protein binding ($K_P 1 - 3 \mu\text{M}$). Only in this very narrow region of the plot a transition to a higher AUC area (i.e. from green→yellow→red) would be predicted if K_P increases, which could lead to an increase in exposure and pharmacodynamic effect leading to a clinical safety concern.

A further example of potential utility may also be improving our understanding of the use of antibodies (Ab) directed against plasma antigens. Here non-intuitive phenomena have also been reported, such as for HA-1A anti-endotoxin antibody (Quezado et al., 1993). The hypothesis investigated in this paper was that an Ab designed to bind endotoxin in plasma would remove the driver of the potentially lethal toxic shock response, in turn improving outcome. In a canine model of endotoxic shock, Quezado et al. (1993), reported that an anti-endotoxin Ab antibody actually potentiated the toxic shock. This may be explained by other factors. However the current work highlights that the theoretical risk of potentiation exists in these circumstances, if one assumes that Ab could be interchanged with plasma protein. With information on binding to molecular target, Ab pharmacokinetics and on the elimination of the molecule, the risks could easily be explored. Conversely, this phenomenon could be exploited to improve the pharmacokinetic–pharmacodynamic (PKPD) properties of drugs. For example, these conclusions suggest that an Ab designed to bind a small molecule drug with optimal affinity could improve the PKPD properties of that drug. Indeed there have been reports in the literature of this application in preclinical species (Lobo et al., 2003).

The work outlined in this paper provides the mathematical tools to define the parameters required for success. The model presented is necessarily a simplification of human physiology and for the purposes of this manuscript we have assumed application to drugs with restricted distribution, representing a subset of total drug property space. However, Hollósy et al., 2006, have shown that the

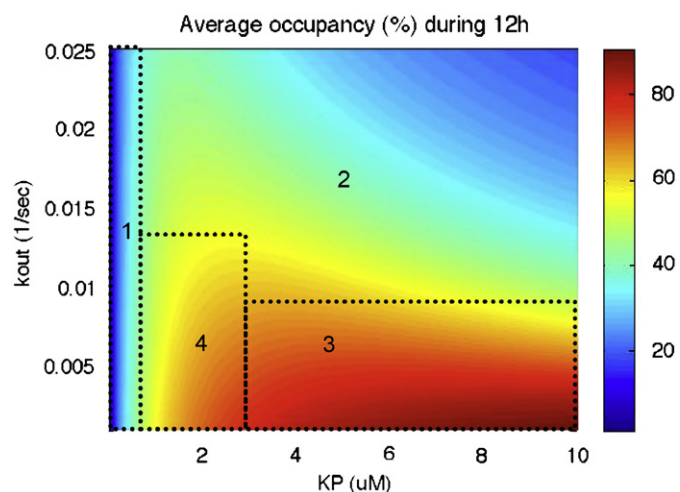


Fig. 7. Contour plot illustrating the relationship between target occupancy (expressed as average receptor occupancy ($T^{-1}AUC(T)$) over $T = 12$ h and k_{out} and K_P . Values of $AUC(T)$ were calculated using Eq. (7.18) with the following parameter values: $T = 12$ h; $P_0 = 750 \mu\text{M}$; $b = 1000$. Regions 1–4 marked by the dotted lines are described in the text.

volume of distribution V_d for drugs with a range of physicochemical properties can be estimated via measures of binding to plasma protein and phospholipid. This raises the potential that the model may be more generically applicable to include drugs with higher observed V_d , by having P represent phospholipid and K_P affinity for binding to phospholipid. Further exploration of this hypothesis would be an interesting next step in this research.

In conclusion, in this paper we have presented a quantitative framework for incorporating the impact of plasma-protein binding into PKPD models. This should assist in the rational design in medicinal chemistry drug discovery programs.

Appendix A. Justification of the reduced system (5.5) on the short time scale

We write the system (5.3) as

$$\begin{cases} \frac{dx}{d\tau_1} = az - (az + 1)x \\ \frac{dy}{d\tau_1} = \rho_y \\ \frac{dz}{d\tau_1} = (az + 1)\frac{P_0}{I_0}x - a\frac{P_0}{I_0}z + \rho_z \end{cases} \quad (A.1)$$

where

$$\rho_y = \varepsilon\{bz - (bz + 1)y\} \quad \text{and} \quad \rho_z = \varepsilon\{bz + 1\}\frac{R_0}{I_0}y - \left(\varepsilon b\frac{R_0}{I_0} + \frac{k_{out}}{k_{-1}}\right)z \quad (A.2)$$

and we estimate the remainder terms ρ_y and ρ_z .

A.1. $k_{-1} = 10^3 \text{ s}^{-1}$:

In view of the constants in Tables 1 and 2, we have:

$$|\rho_y| = \varepsilon|bz(1 - y) - y| < \varepsilon(b + 1) < 2 \times 10^{-3} \quad (A.3)$$

As to ρ_z , we have

$$\varepsilon\{bz + 1\}\frac{R_0}{I_0} < 2 \times 10^{-5} \quad \text{and} \quad \varepsilon b\frac{R_0}{I_0}z \leq 10^{-5}$$

and if k_{out} ranges from 10^{-2} to 10^{-1} s^{-1} , then k_{out}/k_{-1} ranges from 10^{-5} to 10^{-4} . Therefore,

$$|\rho_z| < 2 \times 10^{-4} \quad (A.4)$$

We deduce from (A.3) that, since $y(0) = 0$,

$$y(\tau_1) < 2 \times 10^{-3}\tau_1 \quad \text{for} \quad \tau_1 > 0$$

i.e., for times τ_1 of order unity, we may approximate y by

$$y(\tau_1) = 0$$

Similarly, from (A.4) we conclude that x and z may be approximated for $\tau_1 = O(1)$ by the solution of the two-dimensional system

$$\begin{cases} \frac{dx}{d\tau_1} = az - (az + 1)x \\ \frac{dz}{d\tau_1} = (az + 1)\frac{P_0}{I_0}x - a\frac{P_0}{I_0}z \end{cases} \quad (5.7)$$

A.2. $k_1 = 10 \mu\text{M}^{-1} \text{ s}^{-1}$:

For $1 \leq k_{-1} \leq 10^3 \text{ s}^{-1}$ we have $\varepsilon \leq 10^{-3}$ so that

$$\varepsilon\{bz + 1\}\frac{R_0}{I_0} < 1.001 \times 10^{-2} \quad \text{and} \quad \varepsilon b\frac{R_0}{I_0}z \leq 10^{-2}$$

Therefore, the dynamics of x and z described by (5.3) is well approximated by the dynamics of (5.7) as long as $\tau_1 = O(1)$.

Appendix B. Justification of the reduced system (5.7) on the medium time scale

In order to justify the reduced system (5.7) we need to estimate the remainder term ρ_z in (A.1), defined in (A.2), under the assumption that $x = \bar{x}$ and $z = \bar{z}$. Since $\bar{z} < \kappa$ we now find that

$$\varepsilon\{bz + 1\}\frac{R_0}{I_0} \leq 10^{-5}\kappa \quad \text{and} \quad \varepsilon b\frac{R_0}{I_0}z \leq 10^{-5}\kappa$$

and if k_{out} ranges from 10^{-2} to 10^{-1} s^{-1} , then $k_{out}\bar{z}/k_{-1}$ ranges from $10^{-5}\kappa$ to $10^{-4}\kappa$.

Since the half time $\tau_{1,1/2}^*$ computed in (6.4) amounts to around $10^3\kappa^{-1}$, it follows that on the medium time scale the remainder term ρ_z will be small, so that on that time scale the reduction of (A.1) to the system (5.7) is justified. We recall that (\bar{x}, \bar{z}) is an equilibrium point of the system (5.7). Therefore, since—after a brief initial adjustment—the orbit starts at this point, it follows that the solution (\bar{x}, \bar{z}) is given by

$$\bar{x}(\tau_1) = \bar{x} \quad \text{and} \quad \bar{z}(\tau_1) = \bar{z}$$

and hence, that for the medium time scale the solution (x, z) is close to (\bar{x}, \bar{z}) , i.e.,

$$x(\tau_1) \approx \bar{x} \quad \text{and} \quad z(\tau_1) \approx \bar{z}$$

Appendix C. A phase plane argument

In this appendix we prove that after $y(t)$ and $z(t)$ have reached their plateau values \bar{y} and \bar{z} , we have

$$y(t) < \bar{y} \quad \text{and} \quad z(t) < \bar{z} \quad (C.1)$$

In terms of the scaled time τ_3 defined in (7.9) the dimensionless concentrations of the receptor complex y and the inhibitor z satisfy the reduced system

$$\begin{cases} \kappa \frac{dy}{d\tau_3} = bz - (bz + 1)y \\ \frac{dz}{d\tau_3} = v(bz + 1)y - (bv + \theta)z \end{cases} \quad v = \frac{R_0}{I_0}, \quad \theta = \frac{k_{out}}{k_{-2}} \quad (7.10)$$

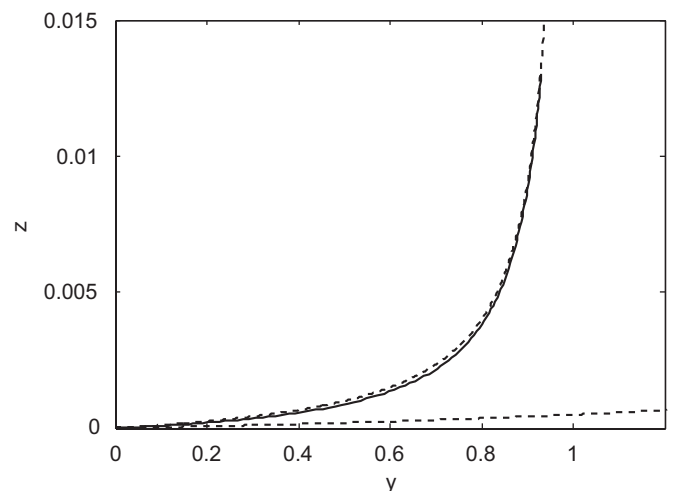


Fig. 8. Orbit in the (y, z) -plane of the solution $(y(\tau_3), z(\tau_3))$ of the system (7.10) which starts at (\bar{y}, \bar{z}) (solid) as well as the null clines Γ_y and Γ_z (dotted). Note that (\bar{y}, \bar{z}) lies on Γ_y and that the orbit lies below Γ_y for all $\tau_3 > 0$ and follows it very closely. Here $K_P = 10 \mu\text{M}$ and $k_{out} = 0.02$.

in which the constant b is defined in (5.2), κ in (5.12) and v and θ in (7.10). We prove (C.1) by means of a phase plane argument for this system.

The null clines of this system, i.e. the curves in the (z, y) plane on which $dy/d\tau_3 = 0$, respectively, $dz/d\tau_3 = 0$ are given by

$$\Gamma_y : y = \frac{bz}{bz+1} \quad \text{and} \quad \Gamma_z : y = \frac{bz}{bz+1} \left(1 + \frac{\theta}{bv}\right) \quad (\text{C.2})$$

In Fig. 8 we show the solution of the system (7.10) which starts at the point (\bar{y}, \bar{z}) . By (6.3), this point lies on the null cline Γ_y and hence for $\tau_3 > 0$ and small, the orbit lies below Γ_y . Since the vector field on Γ_y points downward, the orbit can never cross Γ_y again. Therefore, both $y' < 0$ and $z' < 0$ for all $\tau_3 > 0$, which proves the two inequalities in (C.1).

References

- Benet, L.Z., Hoener, B., 2002. Changes in plasma protein binding have little clinical relevance. *Clin. Pharmacol. Ther.* 71, 115–121.
- Copeland, R.A., Pompliano, D.L., Meek, T.D., 2006. Drug-target residence time and its implications for lead optimization. *Nat. Rev. Drug Discov.* 5, 730–739.
- Ericsson, H., Hamren, B., Bergstrand, S., Elebring, M., Fryklund, L., Heijer, M., Öhman, K.P., 2004. Pharmacokinetics and metabolism of tesaglitazar, a novel dual-acting peroxisome proliferator-activated receptor α/γ agonist, after single oral and intravenous dose in humans. *Drug Metab. Dispos.* 32, 929–932.
- Fournier, T., Medjoubi, N.N., Porquet, D., 2000. Alpha-1-Acid Glycoprotein. *Biophys. Acta* 1482, 157–171.
- Frostell-Karlsson, A., Remaeus, A., Roos, H., Andersson, K., Borg, P., Hämäläinen, M., Karlsson, R., 2000. Biosensor analysis of the interaction between immobilized human serum albumin and drug compounds for prediction of human serum albumin binding levels. *J. Med. Chem.* 18 43 (10), 1986–1992.
- Gerskowitch, V.P., Hodge, J., Hull, R.A.D., Shankley, N.P., Kalindjian, S.B., McEwen, J., Black, J.W., 2007. Unexpected relationship between plasma protein binding and the pharmacodynamics of 2-NAP, a CCK1-receptor antagonist. *Br. J. Clin. Pharmacol.* 63 (5), 618–622.
- Hollósy, F., Valkó, K., Hersey, A., Nunhuck, S., Kéri, G., 2006. Estimation of volume of distribution in humans from high throughput HPLC-based measurements of human serum albumin binding and immobilized artificial membrane partitioning. *J. Med. Chem.* 49, 6958–6971.
- Israïli, Z.H., Dayton, P.G., 2001. Human Alpha-1-Glycoprotein and its interactions with drugs. *Drug Metab. Rev.* 33, 161–235.
- Jusko, W.J., 1976. Plasma and tissue protein binding of drugs in pharmacokinetics. *Drug Metab. Rev.* 5, 43–140.
- Kenakin, T., 2004. *A Pharmacology Primer: Theory, Application and Methods*. Elsevier Academic Press.
- Lobo, E.D., Soda, D.M., Balthasar, J.P., 2003. Application of pharmacokinetic-pharmacodynamic modeling to predict the kinetic and dynamic effects of anti-methotrexate antibodies in mice. *J. Pharmacol. Sci.* 92, 1665–1676.
- Martin, B.K., 1965. Kinetics of elimination of drugs possessing high affinity for the plasma proteins. *Nature* 207, 959–960.
- Oie, S., Tozer, T.N., 1979. Effect of altered plasma protein binding on apparent volume of distribution. *J. Pharm. Sci.* 68, 1203–1205.
- Putnam, F.W., 1984. *The Plasma Proteins*, vol. IV, second ed.
- Quezado, Z.M., Natanson, C., Alling, C.D.W., Banks, S.M., Koev, C.A., Elin, R.J., Hosseini, J.M., Bacher, J.D., Danner, R.L., Hoffman, W.D., 1993. A controlled trial of HA-1A in a canine model of gram-negative septic shock. *J. Am. Med. Assoc.* 269, 2221–2227.
- Rich, R.L., Day, Y.S., Morton, T.A., Myszka, D.G., 2001. High-resolution and high-throughput protocols for measuring drug/Human Serum Albumin interactions using BIACORE. *Anal. Biochem.* 296 (2), 197–207.
- Sansom, L.N., Evans, A.M., 1995. What is the true clinical significance of plasma protein binding displacement interactions? *Drug Safety* 12, 227–233.
- Schäfer-Korting, M., Korting, H., Rittler, W., Obermüller, W., 1995. Influence of serum protein binding on the *in vitro* activity of antifungal agents. *Infection* 23, 292–297.
- Schuhmacher, J., Kohlsdorfer, C., Böhner, K., Brandenburger, T., Kruk, R., 2004. High-throughput determination of the free fraction of drugs strongly bound to plasma proteins. *J. Pharmacol. Sci.* 93, 816–830.
- Smith, D.A., van de Waterbeemd, H., Walker, D.K., 2006. Pharmacokinetics and metabolism in drug design. In: *Methods and Principles in Medicinal Chemistry*, vol. 31. Wiley-VCH, Weinheim.
- Talbert, A.M., Tranter, G.E., Holmes, E., Francis, P.L., 2002. Determination of drug-plasma protein binding kinetics and equilibria by chromatographic profiling: Exemplification of the Method Using L-Tryptophan and Albumin. *Anal. Chem.* 74, 446–452.
- Trainor, G.L., 2007. The importance of plasma protein binding in drug discovery. *Expert Opin. Drug. Discov.* 2, 51–64.
- Wanwimolruk, S., Birkett, D.J., Brooks, P.M., 1983. Structural requirements for drug binding to site II on Human Serum Albumin. *Mol. Pharmacol.* 24, 458–463.